A Spectroscopic Study of the Epidermal Ultraviolet Chromophore *trans*-Urocanic Acid

Kerry M. Hanson, Bulang Li, and John D. Simon*

Contribution from the Department of Chemistry and Biochemistry, University of California, San Diego, 9500 Gilman Drive, La Jolla, California 93093-0341

Received October 1, 1996[⊗]

Abstract: Photoacoustic calorimetry and steady-state spectroscopic techniques are used to investigate the wavelength-dependent photoreactivity of *trans*-urocanic acid under representative physiological conditions *in vitro*. The maxima of the emission and excitation spectra and the value of $\Delta_r H$, the reaction enthalpy as determined from photoacoustic measurements, varied as a function of the excitation wavelength. From these data, we are able to confirm that the photolysis of *trans*-UA at 266 nm (the peak of the absorption spectrum where isomerization is inefficient) generates a long-lived electronically excited triplet state that lies approximately 230 kJ/mol above the ground state. Isomerization does not occur from this triplet electronic state, but bimolecular energy transfer to O_2, generating $^1\Delta_g$ (O_2), does occur. Excitation of *trans*-UA at 308 nm (in the tail of the absorption spectrum) does not lead to triplet state formation. Instead, excitation at this wavelength leads to isomerization. Using measured isomerization quantum yields at this photolysis wavelength ($\Phi = 0.49$), we are able to determine that the ground state of *cis*-UA lies about 40 kJ/mol above that of the *trans* isomer. Photoacoustic data recorded following the photolysis of *cis*-UA at 266 and 308 nm show the same trends, supporting the conclusion that the wavelength-dependent chemistry is not due to the presence of multiple ground-state rotamers. The data indicate that the broad structureless absorption spectrum of *trans*-UA is comprised of overlapping transitions due to at least two distinct electronic states. The different reactivities of these two states result in the wavelength-dependent isomerization yields that have been measured for *trans*-UA in the UV-B (280−320 nm) range.

Introduction

Overwhelming evidence indicates that excess exposure to the sun's ultraviolet (UV) radiation suppresses the immune response, which promotes tumor growth and the risk of skin cancer.[1] Current trends in photocarcinogenesis research postulate UV-induced immunesuppression in the skin begins in the epidermis when UV is absorbed by particular chromophores.[2] Recently, the epidermal ultraviolet chromophore urocanic acid (UA) has received considerable attention because of its immunomodulatory behavior.

UA exists as its *trans* isomer (approximately 30 μg/cm^2; *t*-UA) in the uppermost layer of the skin (stratum corneum), which is formed as the cells of the second layer become metabolically inactive. During this process proteins and membranes degrade, histidine is released, and histidase (histidine ammonia lyase) catalyzes the deamination of histidine to form *t*-UA. Due to an absence of epidermal urocanase that could metabolize UA further, *t*-UA accumulates in the epidermis until removal by either the monthly skin renewal cycle or through sweat.[2]

Upon absorption of ultraviolet radiation, the naturally occurring *t*-UA isomerizes to its *cis* form (*c*-UA; Scheme 1, neutral molecule), which absorbs in the UV as well (Figure 1). Because DNA lesions (e.g., pyrimidine dimers in the p53 gene) in basal epidermal cells can result by UV-B absorption (280−320 nm),[4] initial research proposed that UA acted as a natural sunscreen absorbing UV-B in the stratum corneum before the damaging rays could penetrate into lower epidermal zones.[5] However, since De Fabo and Noonan's pioneering work[6] that showed the

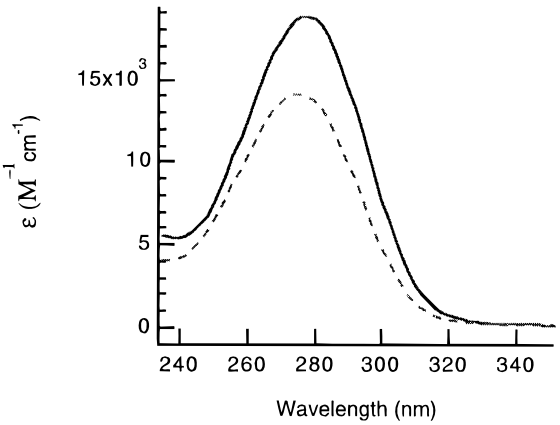

Figure 1. Absorption spectra of *trans*- and *cis*-urocanic acid (pH 7.2). Both isomers absorb in the UV-B with *cis*-UA (dashed line) having a smaller molar extinction coefficient ($\epsilon = 13\,600$ at 277 nm) relative to the naturally occurring *trans*-UA isomer (solid line, $\epsilon = 18\,800$ at 277 nm).[3]

Scheme 1

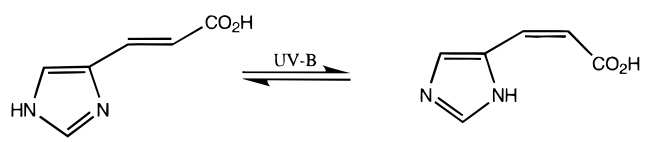

trans-Urocanic Acid *cis*-Urocanic Acid

* Author to whom correspondence should be addressed.

[⊗] Abstract published in *Advance ACS Abstracts,* February 15, 1997.

(1) National Institutes of Health Consensus Development Conference Statement **1989**, *7*, 1−10.

(2) Norval, M.; Gibbs, N. K.; Gilmour, J. *Photochem. Photobiol.* **1995**, *62*, 209−217.

(3) Hug, D. H.; Hunter, J. K. *Photochem. Photobiol.* **1994**, *59*, 303−308.

(4) Ziegler, A.; Jonason, S.; Leffell, D. M.; Simon, J. A.; Sharma, H. W.; Kimmelman, J.; Remington, L.; Jacks, T.; Brash, D. E. *Nature* **1994**, *372*, 773−776.

(5) Zenisek, A.; Kral, J. A.; Hais, I. M. *Biochim. Biophys. Acta* **1955**, *18*, 589−591.

S0002-7863(96)03440-3 CCC: $14.00

action spectrum for immunosuppression of contact hypersensitivity overlapped that of the absorption spectrum for UA, researchers have found that *c*-UA suppresses contact hypersensitivity and delayed hypersensitivity, reduces the Langerhans cell count in the epidermis, prolongs skin graft survival time, and affects natural killer cell activity.[2,7−12] Because *c*-UA has shown such immunomodulatory behavior, it is now postulated to act as a mediator for UV-induced immune suppression.

Photochemically, urocanic acid is an unusual molecule because the isomerization quantum yield of *t*-UA and thereby the subsequent accumulation of *c*-UA is wavelength dependent. The isomerization efficiency (Φ) peaks at 310 nm (the red edge of the absorption spectrum) ($\Phi = 0.49$) but is greatly reduced near the absorption maximum (at 266 nm $\Phi = 0.05$).[13] Arguments used to explain urocanic acid's wavelength-dependent isomerization include photosensitization by other chromophores,[14] high *t*-UA concentration,[15] and *t*-UA association with other epidermal proteins.[16] Generally, wavelength-dependent photochemistry arises from an intrinsic characteristic of the molecule: either the presence of multiple ground-state rotamers or electronic states. Most molecules do not exhibit wavelength-dependent photochemistry, although exceptions do exist, and examples include cinnamic acid, diphenylbutadiene, and diphenylhexatriene. Cinnamic acid is known to have multiple electronic states that form different photoproducts upon excitation at variable wavelengths,[17] and the wavelength-dependent photochemistry of diphenylbutadiene[18] and dihexatriene[19] has been explained to result from the presence of different rotamers under the absorption profile. Both multiple ground-state rotamers and electronic states have been proposed to contribute to the wavelength-dependent isomerization of *t*-UA. For example, semiempirical calculations by Shukla and Mishra[20] assigned multiple transitions for different tautomers of *t*-UA, and experiments probing for multiple-electronic states were carried out by Morrison[13] after noting the similarity to cinnamic acid, but no definitive conclusions could be made at that time. In fact, no conclusive experimental evidence currently exists to support either argument. Because this fundamental aspect of the photoreactivity of *t*-UA is not well-understood and because the accumulation of *c*-UA is of such immunological concern, we have carried out detailed spectroscopic investigations of UA under representative physiological conditions (pH 7.2 and pH 5.6, the average pH of sweat), in order to elucidate the nature of the wavelength-dependent isomerization of *t*-UA.

Materials and Methods

Reagents and Sample Preparation. *trans*-Urocanic acid and quinine sulfate were purchased from Aldrich (Milwaukee, WI) and used without further purification. *t*-UA purity was initially checked by HPLC.[14] *c*-UA was isolated following the procedure of Anglin and Everett.[21] Dowex 1x8-400 ion exchange resin was purchased as the chloride ion from Aldrich and prepared in the acetate form by passing a solution of 12% acetic acid/10% sodium acetate until the solution was free of chloride ions. Separation of the two isomers was achieved using a gradient of 0.04 M acetic acid and confirmed using Whatman thin-layer chromatography cellulose sheets (Fischer; Tustin, CA). Bromocresol purple was purchased from Fischer. All solutions were buffered in either 0.1 M acetate buffer (pH 5.6) or 0.1 M potassium phosphate buffer (pH 7.2).

Absorption. Absorption spectra were recorded on an HP 8245 A diode array spectrophotometer. For spectra acquired at variable temperature between 21 and 80 °C, a jacketed, quartz flow cell (1 cm × 1 cm) cooled or heated by a water circulator (Brinkman Instruments Co.) was used. pH 7.2 buffered, 0.05 mM *t*-UA samples were made for the variable temperature absorption experiments.

Fluorescence. Corrected emission and excitation spectra were recorded on a Spex Industries Fluorolog-2 spectrofluorometer with right angle detection. Because the emission intensity of *t*-UA was found to be very weak, 2 mm excitation and emission slits were used to provide maximum signal intensity with minimal broadening of the excitation wavelength (bandpass = 7.5 nm). Fluorescence samples had an optical density of 0.1 (μM concentrations) in a 1 cm path length quartz fluorescence cell. Relative fluorescence quantum yields (Φ_f) were estimated using the following relationship[22,23]

$$\Phi_F = \Phi_{F,ref}(A_{ref}/A)(n_D/n_{D,ref})2(a/a_{ref}) \quad (1)$$

where a is the area under the emission spectrum, n_D is the index of refraction of the solvent, A is the absorbance, and $\Phi_{F,ref}$ is the known fluorescence quantum yield of a reference compound. Quinine sulfate in 1 N H_2SO_4 was used as the reference compound.[24]

Single Photon Counting. The apparatus has been described in detail elsewhere.[25] An excitation wavelength of 290 nm was used, and the emission at 360 nm from samples in a 1 cm quartz fluorescence cell was collected at a right angle relative to the excitation source. Dilute *t*-UA samples (μM concentrations) were used to prevent aggregation and self-absorption.

Photoacoustic Calorimetry. The experimental design was similar to that described by Peters and co-workers.[26] The signals from the *trans*-UA samples were compared to those from bromocresol purple under identical conditions.[27] Purging the sample with either argon (Ar) or oxygen was done without disturbing the cell apparatus.

The photoexcitation at 308 nm (corresponding to an excitation energy of 390 kJ/mol) was produced by an excimer laser (Lumonics Research LTD). The excitation pulses were 24 ns in duration, and the repetition rate of the laser was 1 Hz. The heat released was detected perpendicular to the excitation source by a PZT transducer (Panametrics A103.S, 1 MHz) attached to the sample cell with a thin layer of silicon grease. The signal was preamplified (Panametrics pre-amp 5660b) and recorded by a digital scope (LeCroy 9450 A) or Transient Digitizer (Biomation Corp.), which was optically triggered by the laser. The data were then transferred to a computer for analysis. The beam diameter at the sample

(6) De Fabo, E. C.; Noonan, F. P. *J. Exp. Med.* **1983**, *157*, 84−98.
(7) El-ghorr, A.; Pierik, F.; Norval, M. *Photochem. Photobiol.* **1994**, *60*, 256−261.
(8) Kurimoto, I.; Streilein, J. W. *J. Immunol.* **1992**, *148*, 3072−3078.
(9) Norval, M.; Simpson, T. J.; Bardshiri, E.; Howie, S. E. M. *Photochem. Photobiol.* **1989**, *49*, 633−639.
(10) Gilmour, J. W.; Norval, M. *Photodermatol. Photoimmunol. Photomed.* **1993**, *9*, 250−259.
(11) Gilmour, J. W.; Vestey, J. P.; George, S.; Norval, M. *J. Invest. Dermatol.* **1993**, *101*, 169−74.
(12) Guymer, R. H.; Mandel, T. E. *Transplantation* **1993**, *55*, 36−43.
(13) Morrison, H.; Bernasconi, C.; Pandey, G. *Photochem. Photobiol.* **1984**, *40*, 549−550.
(14) Morrison, H.; Avnir, D.; Bernasconi, C.; Fagan, G. *Photochem. Photobiol.* **1980**, *32*, 711−714.
(15) Gibbs, N. K.; Norval, M.; Traynor, N.; Wolf, M.; Johnson, B. E.; Crosby, J. *Photochem. Photobiol.* **1993**, *57*, 584−590.
(16) Stab, F.; Hoppe, U.; Sauermam, G. *J. Invest. Dermatol.* **1994**, *102*, 666.
(17) Ullman, E. F.; Babad, E.; Sung, M. *J. Am. Chem. Soc.* **1969**, *91*, 5792−5797.
(18) Wallace-Williams, S. E.; Moller, S.; Goldbeck, R. A.; Hanson, K. M.; Lewis, J. W.; Yee, W. A.; Kliger, D. S. *J. Phys. Chem.* **1993**, *97*, 9587−9592.
(19) Saltiel, J.; Sears, D. F.; Sun, Y.-P.; Choi, J.-O. *J. Am. Chem. Soc.* **1992**, *114*, 3607−3612.
(20) Shukla, M. K.; Mishra, P. C. *Spectrochim. Acta* **1995**, *51A*, 831−838.
(21) Anglin, J. H.; Everett, M. A. *Biochimica Biophysical Acta* **1964**, *88*, 492−501.
(22) Guilbault, G. G. *Practical Fluorescence*; Marcel Dekker: New York, 1973; pp 11−14.
(23) Bridges, J. W. *Standards In Fluorescence Spectrometry*; Miller, J. N., Ed.; Chapman and Hall: New York, 1981; p 75.
(24) Melhruish, W. H. *J. Phys. Chem.* **1961**, *65*, 229.
(25) Farnum, M. F.; Magde, D.; Howel, E. E.; Hirai, J. T.; Warren, M. S.; Grimsley, J. K.; Kraut, J. *Biochemistry* **1991**, *30*, 11567−11579.
(26) Grabowski, J. J.; Simon, J. D.; Peters, K. S. *J. Am. Chem. Soc.* **1984**, *106*, 4515−4516.
(27) Westrick, J. A.; Peters, K. S. *Biochemistry* **1990**, *29*, 6741−6746.

was less than 2 mm, and filters were used to keep the pulse energy around 30.0 ± 0.5 μJ. Between 40 and 80 waveforms were averaged per sample. Sample optical densities were kept at an optical density of 0.30 at the excitation wavelength to within 2% of each other.

Temperature studies were carried out at 308 nm to determine if a change in molecular volume due to isomerization contributed to the overall signal (see data analysis). All experimental parameters were identical to the room temperature studies, except a jacketed flow cell cooled by a water circulator (Brinkman) was used in place of the quartz fluorescence cell in order to control the temperature of the solution. The temperature range that could be accessed was between 9 and 30 °C. The analysis of the signal as a function of temperature followed the protocol developed by Westrick and Peters.[27]

Photoexcitation at 266 nm (450 kJ/mol) was accomplished using a home-built Nd/YLF laser. The excitation pulses were 20 ps in duration operating at 1 KHz. Signal amplification and digitization and sample optical density were identical to those used in the 308 nm excitation experiments. The pulse energy used was on the order of 10.0 μJ.

Photoacoustic Calorimetry Data Analysis.[28] Absorption of light by a molecule causes an increase in its internal energy and, potentially, its volume (from conformational changes). Part, or all, of this energy can, in turn, be transferred to the solvent. As the solvent expands from this energy transfer, an acoustic wave is generated; the amplitude of the wave is related to the quantum yields for the nonradiative decay pathways accessible to the excited molecule. The signal amplitude, S, is a function of ΔV_{th}, the change in volume due to thermal expansion, and ΔV_{con}, the change in molecular volume of the system

$$S = K(\Delta V_{th} + \Delta V_{con}) \tag{2}$$

K is a constant unique to the instrument response function which relates the amount of heat released to the cell geometry.

For most reactants ΔV_{con} contributes little to the signal and ΔV_{th}, the thermal expansion contribution, dominates. However, the isomerization of UA could cause a change in molecular volume, which would lead to a contribution of ΔV_{con} to the signal. By studying the temperature-dependence of the photoacoustic signal, it is possible to determine if there is any significant contribution from ΔV_{con}.

The thermal contribution to the signal is given by

$$\Delta V_{th} = (\beta/C_p\rho)Q \tag{3}$$

where Q is the thermal energy released from the reactant, β is the thermal expansion coefficient of the solvent, C_p is the heat capacity of the solvent, and ρ is the density of the solvent. The photoacoustic signal can therefore be expressed as

$$S = K((\beta/C_p\rho)Q) + \Delta V_{con} \tag{4}$$

For a compound like bromocresol purple, which is known to both convert all the absorbed energy into heat and undergo a negligible molecular volume change ($\Delta V_{con} = 0$), the photoacoustic signal is given by

$$S_{ref} = K(\beta/C_p\rho)E_{h\nu} \tag{5}$$

where $E_{h\nu}$ is the photon energy. The ratio of S (the heat released by an arbitrary molecule) relative to S_{ref} (the heat released by a reference molecule such as bromocresol purple), ϕ, is then

$$\phi = S/S_{ref} = Q/E_{h\nu} + \Delta V_{con}/(\beta/C_p\rho)E_{h\nu} \tag{6}$$

Rearranging eq 6 gives

$$\phi E_{h\nu} = Q + \Delta V_{con}/(\beta/C_p\rho) \tag{7}$$

For our experimental conditions, we can assume that Q and ΔV_{con} are temperature dependent.[27] The variables ϕ and $\beta/C_p\rho$ to the signal, then a plot of $\phi E_{h\nu}$ versus $(\beta/C_p\rho)^{-1}$ will yield a slope and intercept of ΔV_{con} and Q, respectively. For the specific case of *t*-UA, isomerization does not significantly affect the molecular volume (*vida infra*), and we find that any contribution due to molecular volume expansion is negligible relative to the thermal expansion. The nonradiative heat released by *t*-UA, Q, is then easily from

$$\phi = S/S_{ref} = Q/E_{h\nu} \tag{8}$$

and $\Delta_r H$, the reaction enthalpy is approximated by

$$\Delta_r H = E_{h\nu} - Q \tag{9}$$

Results

Absorption and Emission Spectroscopy. Figure 1 displays the absorption spectra of *cis*- and *trans*-UA at pH 7.2. The spectra of the two isomers have similar shapes with extinction coefficients at 278 nm of 13 600 and 18 800 for the *cis*- and *trans*-isomers, respectively.[3] Note that the molecular structure of UA varies with pH (see Figure 2) because of the acidity of the carboxylic acid and imidazole protons. Mehler and Tabor[29] determined the pK_a of the three protonation sites on this molecule to be pK_a = 3.5 for the carboxylic hydrogen, pK_a = 5.8 for the tertiary imidazole nitrogen, and pK_a = 13 for the secondary imidazole nitrogen. These workers concluded that deprotonation of the carboxylic and the imidazole groups causes the electronic absorption spectrum to shift to lower energy. At pH 7.2, the absorption spectrum of *t*-UA maximizes at 278 nm, a red shift of about 10 nm compard to the *t*-UA spectrum at pH 5.6 (see Figure 2). We also examined the absorption spectrum of *t*-UA as a function of temperature for a solution pH of 7.2. The red edge of the absorption spectrum was found to be temperature independent over the range from 21.7 to 76.5 °C.

The emission spectra for *trans*-UA in two different pH solutions are shown in Figure 2. The molecular structure at the corresponding pH is also displayed. The background buffer emission and the strong water Raman band have been subtracted from the data. Because the emission is weak and because of the intense Raman band, an accurate determination of the radiative quantum yield was difficult. We estimate that Φ_f is less than 10^{-4} for excitation of *t*-UA at 266 nm and that Φ_f is less than 10^{-3} for excitation of *t*-UA between 300 and 310 nm. These maximum yields were determined by comparing the intensity of the emission of *t*-UA to that of the standard quinine sulfate.

As the data in Figure 2 show, the excitation of *t*-UA at 266 nm yields emission maximum at 354 nm, which is blue shifted relative to emission maximum measured for the excitation of *t*-UA at 310 nm. This result is independent of the pH of the solution. Another interesting trend is seen by comparing the emission for excitation at the red edge of the absorption spectrum for the two different pHs studied. With increasing pH, the emission maximum shifts to higher energy. Excitation of a pH 5.6 solution of *t*-UA at 310 nm yields emission that has a maximum intensity at 386 nm, but excitation of a pH 7.2 solution of *t*-UA yields emission that has a maximum intensity at 370 nm.

We attempted to determine the excited state lifetime for the two different *t*-UA solutions by time-resolved single photon counting. The lifetime of the emission was found to be shorter than the instrument response (40 ps; data not shown).

The excitation spectra for pH 5.6 and pH 7.2 *t*-UA solution were also examined (data not shown). The data show that the maximum of the excitation spectrum peaks at 280 nm for emission collected at 360 nm for pH 5.6 *t*-UA (recall that the tertiary nitrogen is protonated at this pH). Similar results were found for *t*-UA at pH 7.2—a pH where the tertiary nitrogen is deprotonated.

(28) Peters, K. S. *Angew. Chem., Int. Ed. Engl.* **1994**, *33*, 294−302.
(29) Mehler, A. H.; Tabor, H. *J. Biol. Chem.* **1955**, *201*, 775−784.

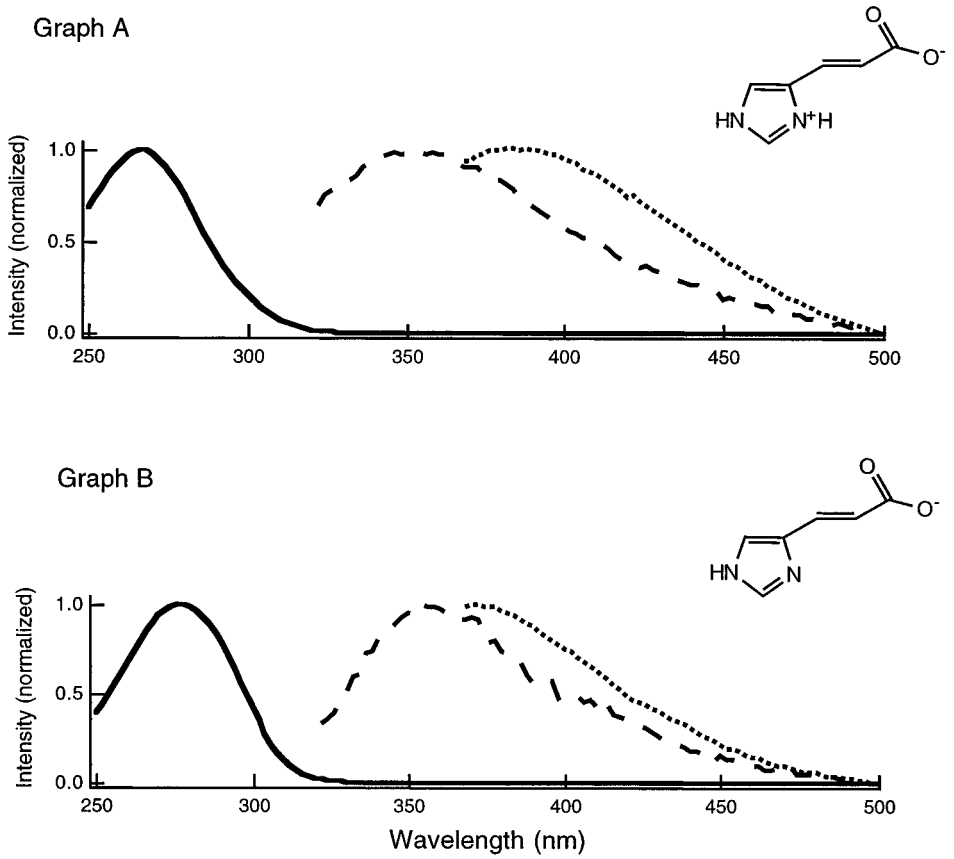

Figure 2. Absorption and emission spectra acquired for *t*-UA at pH 5.6 (graph A) and at pH 7.2 (graph B) as a function of excitation wavelength: (—) *t*-UA absorption spectrum, (- -) emission from 310 nm excitation; and (— —) emission from 266 nm excitation. Note that the absorption spectrum shifts to lower energy when the tertiary nitrogen is deprotonated and that the emission maximum depends upon the excitation wavelength.

Photoacoustic Calorimetry. Figure 3A shows the photoacoustic signal following excitation of *t*-UA (pH 7.2, 0.1 M phosphate buffer) at 266 nm in both saturated argon (Ar) and oxygen solutions. The signal from the reference compound bromocresol purple is also shown. The signals from the *t*-UA solutions are slightly shifted from that of the reference sample. Kinetic information can be derived from such time shifts;[28] however, we have not calculated transient lifetimes from these data, because the shifts are small and often not consistent.

The signal for the reference compound is independent of pH and therefore all *t*-UA signals were compared to bromocresol purple at pH 5.6 (0.1 M acetate buffer). At both pH 7.2 and pH 5.6 the amount of heat released by *t*-UA is identical, within the signal to noise. Approximately 49% of the energy absorbed is released nonradiatively by *t*-UA when either solution is saturated with Ar. The excited molecule therefore retains about 230 kJ/mol on the time scale of this measurement. In comparison, 63% of the absorbed energy is released when the solution is saturated with O_2 instead of argon.

Figure 3B shows the photoacoustic signal of *t*-UA (pH 7.2, 0.1 M phosphate buffer) following photolysis at 308 nm for both argon and oxygen saturated solutions. Once again the reference signal from a bromocresol purple solution is also shown. Unlike the photoacoustic data recorded for the excitation of *t*-UA at 266 nm, the signal shown in Figure 3B shows no difference in intensity for the argon or O_2 saturated solutions. In addition, almost all of the energy absorbed is released as heat. Only 40 kJ/mol is retained by the molecule.

Figure 4 (parts A and B) show the photoacoustic signal for *c*-UA (pH 7.2, 0.1 M phosphate buffer) following excitation at 266 and 308 nm, respectively, compared to the reference. The *c*-UA data exhibit nearly identical wavelength-dependent behavior to that of *t*-UA. At 266 nm under argon atmosphere, approximately 51% of the heat is retained by the molecule, which corresponds to 230 kJ/mol, and 74% of the absorbed energy is released when the solution is saturated with O_2 instead of argon. At 308 nm, like *t*-UA, *c*-UA releases essentially all of the absorbed energy back to the solvent (>99%).

Discussion

The wavelength-dependent photochemistry of *t*-UA manifests itself in the wavelength-dependent photoacoustic signals, emission, and excitation spectra. The absorption spectrum of *t*-UA and *c*-UA are similar and have no structure and, therefore, shed little insight into the origin of this wavelength-dependent behavior. The emission spectra, on the other hand, provide insight through their excitation wavelength dependence. Specifically, at pH 7.2 excitation at 266 and 310 nm results in emission spectra that maximize at 354 and 370 nm, respectively. Similar shifts are observed for pH 5.6 *t*-UA. The emission spectrum maximizing at 354 nm is insensitive to pH and excitation wavelengths from 260 to 285 nm. The red-shifted spectrum peaks at 386 nm at a pH of 5.6, a 16 nm red shift, and this maximum changes as the excitation wavelength is varied between 300 to 320 nm. The lifetime of the emission following excitation at 290 nm is less than 40 ps (the instrument response) at both pHs indicating that UA undergoes a rapid nonradiative process, which we shall show is due to intersystem crossing from the singlet to the triplet manifold. We now discuss two models consistent with the wavelength-dependent photochemistry. First, the broad and structureless UV spectrum could be due to the presence of multiple ground-state rotamers that have

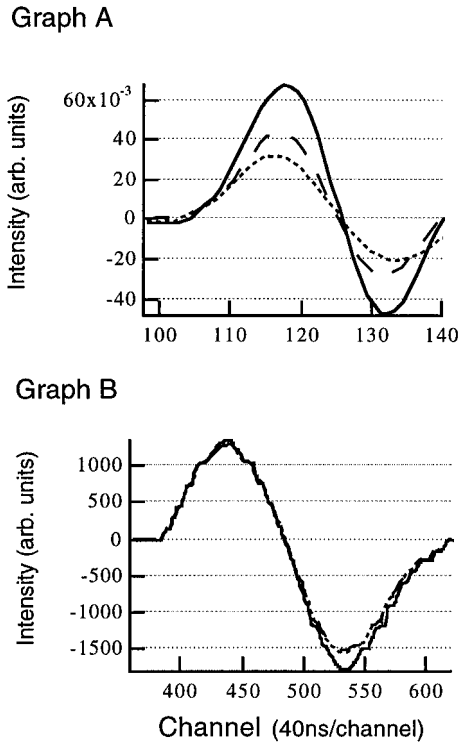

Figure 3. Photoacoustic calorimetry signal of bromocresol purple (reference) and *t*-UA, pH 7.2 collected at variable excitation wavelength, graph A, 266 nm excitation and graph B; 308 nm excitation: (—) reference, (- -) *t*-UA under argon atmosphere, and (— —) *t*-UA under oxygen atmosphere. The signal for *t*-UA excited at 266 nm under argon is approximately half of the reference signal and increases in the presence of oxygen. The signal for *t*-UA excited at 308 nm shows no oxygen affect, and essentially all of the absorbed energy is released back into the solvent under either atmosphere.

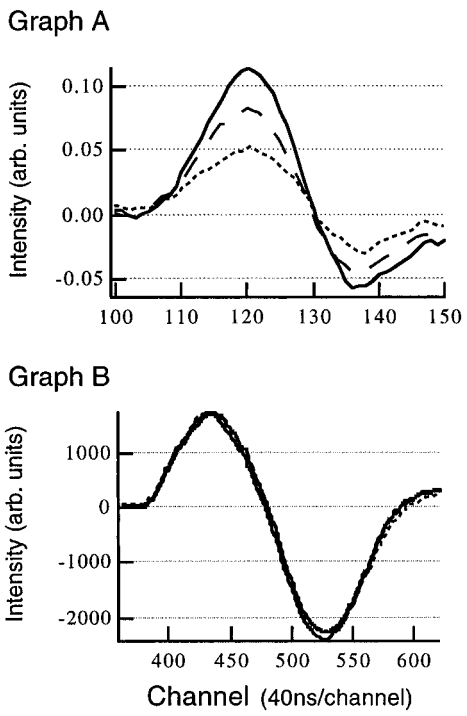

Figure 4. Photoacoustic calorimetry signal of bromocresol purple (reference) and *c*-UA, pH 7.2 collected at variable excitation wavelength, graph A, 266 nm excitation and graph B, 308 nm excitation: (—) reference; (- -) *c*-UA under argon atmosphere, and (— —) *c*-UA under oxygen atmosphere. The data for *c*-UA are essentially the same as those obtained for *t*-UA (see Figure 3).

different absorption spectra, different emission spectra, and different excited state reactivities. Such a model has been used to describe the wavelength-dependent behavior of diphenylbutadiene[18] and dihexatriene.[19] Second, the absorption spectrum of *t*-UA could reflect the superposition of multiple absorption transitions. The different excited states accessed at different excitation wavelengths would then have different reactivities. Such a model has been used to describe the behavior of cinnamic acid.[17] In fact, Morrison's original work on *t*-UA suggested that the wavelength-dependent isomerization yields he determined could potentially arise from multiple electronic states similar to cinnamic acid.[13]

While the electronic transition(s) responsible for UA's absorption in the UV are not assigned, multiple transitions for different tautomers of UA have been calculated by Shukla and Mishra[20] using semiempirical techniques. In their study, the wavelength-dependent photoisomerization is discussed in terms of different tautomers each of which has a different excited electronic state, but the various ground states are close in energy and therefore populated at room temperature. Quantum chemical calculations of nonionic structures of UA have been reported by Lahti *et al.*[30] Both semiempirical and all-electron *ab initio* calculations were carried out in order to calculate the ground-state potential energy surface. Though these two theoretical studies arrive at the same molecular geometry for the most favorable structure of *t*-UA, they differ in the energies associated between the s-trans, s-cis *t*-UA conformers. For example, the calculations of Shukla and Mishra show this difference is approximately 1.3 kJ/mol, which is surmountable by thermal activation at room temperature if we assume that the calculated energy difference between the two conformers is roughly that of the rotational barrier. The study by Lahti *et al.*, however, report that the two conformers differ by about 8.3 kJ/mol. This separation is larger than that calculated by Shukla and Mishra, and the difference was attributed to the inclusion of conjugation effects that result in an increase in the bond-order of the C—C bond.

These calculations do not account for the protonation state of the imidazole group for different pH values (pH 5.6—7.2). Our data indicate that *t*-UA exhibits identical wavelength-dependent photochemistry regardless of pH (5.6—7.2). This means that if the wavelength dependence arises from the presence of ground-state rotamers having different photoreactivities than the relative energies of these rotamers must be insensitive to the protonation of the tertiary nitrogen on the imidazole ring. We also observe that the absorption spectrum of *t*-UA is insensitive to temperature, in contrast to what might be expected if there were several different rotamers contributing to the spectrum, as seen for diphenylbutadiene.[31] Finally, we examined the wavelength-dependent photoacoustic signals following the excitation of *c*-UA at 308 and 266 nm. Unlike *t*-UA, at pH 5.6, the energy difference between rotamers (e.g., the s-cis, s-trans and s-trans, s-cis) is significant because of the stabilization of the cyclic hydrogen bonded structure (15.2 kJ/mol[30]), and therefore one rotamer should dominate the absorption profile. In fact, the absorption spectrum of both *c*-UA and *t*-UA have the same band shape. And, in this work, we determined that the photoacoustic signals for *c*-UA exhibit a similar wavelength-dependent behavior as *t*-UA, which is significant. If *t*-UA's wavelength-dependence arose from the presence of multiple ground-state rotamers, then we would expect that its

(30) Lahti, A.; Hotokka, M.; Neuvone, K.; Ayras, P. *J. Mol. Struct. (Theochem)* **1995**, *331*, 169—179.

(31) Bunker, C. E.; Lytle, C. A.; Rollins, H. A.; Sun, Y.-P. Manuscript in preparation.

photochemistry would differ from that of *c*-UA, whose photochemical behavior should arise from the presence of just one dominant rotamer. Thus, we propose that the wavelength-dependent photoreactivity of both *c*-UA and *t*-UA does not arise from the presence of multiple ground-state rotamers.

We shall now show that the our data supports the conclusion that the wavelength-dependent photochemistry of *t*-UA is due to the presence of multiple electronic states, with overlapping absorption transitions that are not easily distinguished under the structureless absorption spectrum. Overlapping absorption bands are not uncommon for a molecule like UA. The π- and n-type orbitals can lead to energetically similar $\pi\pi^*$ and $n\pi^*$ states. For example, cinnamic acid, a molecule with a similar structure to UA, is known to have at least two closely spaced electronic states,[17] which have been invoked to explain the origin of its wavelength-dependent photochemistry. For cinnamic acid, a $\pi \rightarrow \pi^*$ transition dominates the absorption profile near 280 nm, and there is a weak $n \rightarrow \pi^*$ transition along the red-edge of the absorption band. Morrison suggested that the absorption spectrum of UA could be similarly assigned.[13] In this work, data have been acquired that support such an assignment.

Following excitation of *t*-UA in a pH 7.2 solution near its absorption maximum (266 nm) in an argon saturated solution, the photoacoustic calorimetry results show that approximately half of the absorbed energy is released nonradiatively, which indicates that the molecule retains 50% of the photon energy for a time period greater than 1 μs (the upper end of the time scale detectable by the photoacoustic method). The increase in the photoacoustic signal amplitude (63% of the excitation energy released as heat) when the solution is saturated with oxygen provides insight into the nature of this long-lived electron state of *t*-UA. The fact that the photoacoustic signal increases in the presence of oxygen indicates that O_2 quenched the excited state of *t*-UA. The ground state of O_2 has a molecular term symbol of $^3\Sigma_g$ and the term symbol of the first excited state is $^1\Delta_g$. The lifetime of the $^1\Delta_g$ state of O_2 in water is on the order of a few microseconds.[32] Subsequently, we conclude that the photoacoustic data are reflecting an energy transfer between the excited UA molecule and O_2 and that the excited state of *t*-UA must be a triplet state. The isomerization yield at this wavelength is small ($\Phi < 0.05$[13]). If we assume that the quantum yield for intersystem crossing is 0.95 and that the triplet lifetime is sufficiently long so that none of the excited-state molecules decay on the time scale of the photoacoustic measurement, then the amplitude of the signal for the argon saturated solution can be used to determine the energy of the triplet state. Carrying out this calculation gives a triplet state energy of 230 kJ/mol (55 kcal/mol), which agrees exactly with the value determined by Morrison *et al*. from triplet sensitization studies.[14]

Both pH 5.6 and pH 7.2 solutions of *t*-UA have identical photoacoustic signals following excitation at 266 nm excitation. These solutions also exhibit identical emission spectra when excited at 266 nm (emission maximum 360 nm) and the isomerization efficiency of t-UA is similar at these two opH values.[14] But the ground state molecular structures of pH 5.6 and pH 7.2 *t*-UA solutions differ (Figure 2). The fact that both pH 5.6 and pH 7.2 *t*-UA solutions exhibit identical photochemistry when *t*-UA is excited near its absorption maximum indicates that a common excited state must be reached in these two cases.

The details of the excited-state dynamics at 266 nm can be inferred from an analysis of the excitation spectrum of *t*-UA at the two pHs studied. As Mehler and Tabor found,[29] *t*-UA solutions at pHs greater than approximately 6 have absorption maxima near 280 nm. This spectrum corresponds to *t*-UA where the tertiary imidazole ($pK_a = 5.8$) is deprotonated. Shukla and Mishra[20] determined, and we confirmed, that the excitation spectrum for both pH 5.6 and pH 7.2 *t*-UA peaks near 280 nm (emission collected at 360 nm). These data indicate that the emitting species in both the pH 5.6 and pH 7.2 solutions is a singlet state of *t*-UA where the tertiary nitrogen on the imidazole is deprotonated. This conclusion also agrees with the fluorescence analysis of Shukla and Mishra. Because the excitation spectrum of *t*-UA at a pH of 5.6 peaks at approximately 280 nm (the absorption maximum for deprotonated UA), *t*-UA at this pH must undergo a rapid proton transfer from the conjugated imidazole ring to the solvent following excitation. This model supports a conclusion that the excited state is a $^1\pi\pi^*$ state. Excitation reduces the electron density on the tertiary nitrogen on the imidazole ring, thereby reducing the excited state pK_a to a value below 5.6. Excitation of pH 7.2 *t*-UA ends up in this same state by direct absorption. The excited singlet state then efficiently intersystem crosses to a triplet state. Studies of the photodynamics of *t*-UA at 266 nm probed by femtosecond absorption spectroscopy confirm this model.[33] The proton transfer occurs on a time scale of less than 200 fs, and the subsequent intersystem crossing occurs with a rate constant of 1.4×10^{11} s^{-1}.

Unlike the data obtained for an excitation wavelength of 266 nm, the photoacoustic calorimetry signal of *t*-UA in a pH 7.2 solution at 308 nm shows that almost all (approximately 99%) of the absorbed energy is released back into the solvent. No time-shifts are observed in the data when compared to the reference compound. Thus, this heat release occurs on a subnanosecond time scale. These results are in contrast to the recent microsecond flash photolysis study reported by Laihia *et al*.[34] in which a long-lived (microsecond) excited state is observed following photolysis of *t*-UA at 308 nm. Recent femtosecond absorption studies[33] show that ground state repopulation occurs with a half-life of 85 ps following excitation of *t*-UA at 306 nm, consistent with the photoacoustic data. The discrepancy between these data and those of Laihia may be due to the larger power levels (60 mJ/pulse) used in the latter study.

Similar photoacoustic results were found at a pH of 5.6 where almost all of the absorbed energy at 308 nm is released into the solvent. Additionally, the emission spectra for both pH 5.6 and pH 7.2 *t*-UA solutions excited at 310 nm are similar, and isomerization yields are reported not to vary with pH at this excitation wavelength.[14] Insight into the excited state at this wavelength can be inferred from observing the weak oscillator strength at 308 nm for UA. Unlike the strong oscillator strength observed at 266 nm, the extinction coefficient at 308 nm is weak for *t*-UA solutions at any pH, which most likely reflects absorption to an $^1n\pi^*$ state, similar to cinnamic acid. The photoacoustic data suggest that the $^1\pi\pi^*$ state populated upon excitation at 266 nm is only weakly coupled to the lower energy excited $^1n\pi^*$ singlet state and that proton transfer to the solvent occurs faster than internal conversion. Following excitation at 308 nm, however, a triplet state is not represented by the data indicating that intersystem crossing is slow compared to isomerization. While isomerization of *t*-UA can be triplet sensitized,[14] our results indicate that under physiological conditions isomerization occurs via the singlet manifold.

Evidence that *t*-UA produces a long-lived electronically excited triplet state upon absorption of UV-B near the peak of

(32) Turro, N. J. *Modern Molecular Photochemistry* Benjamin/Cummings: Menlo Park, 1978; p 588.

(33) Li, B.; Hanson, K. M.; Simon, J. D. *J. Phys. Chem.* In press.

(34) Laihia, J. K.; Lemmetyine, H.; Pasanen, P.; Jansen, C. T. *J. Photochem. Photobiol.* **1996**, *33*, 211−217.

its absorption spectrum raises concerns about the subsequent effects of the excitation of t-UA in the epidermis. Higher-energy wavelengths in the solar UV-B, where *t*-UA efficiently intersystem crosses to its triplet state, should not reach the earth's surface because of absorption by stratospheric ozone. However, a yearly depletion of 1% in the concentration of stratospheric ozone is estimated to result in a 2% increase in the rate of skin cancer incidence. This occurs as a result of the additional erythemal UV penetrating to the earth's surface.[35] Additional UV would not only increase the likelihood of *c*-UA production, which is implicated as a mediator for photocarcinogenesis, but also increase the likelihood of *t*-UA triplet state production in the epidermis as the shorter UV-B wavelengths pass through the stratosphere. Our data show that *t*-UA undergoes energy transfer to produce singlet oxygen following the absorption of UV-B radiation. Singlet oxygen is believed to contribute to cellular damage,[36] and it is possible that this photoreactive pathway contributes to the immunosuppressive characteristics exhibited by urocanic acid. We are completing experiments to determine the quantum yield of singlet oxygen via energy transfer from photoexcited *t*-UA.

Acknowledgment. This work was supported by the General Medicine at Institute of NIH through Grant 5 RO1GM41942. We thank Dr. D. Magde for the use of his Excimer laser and Single Photon Counting apparatus and Dr. R. Tsien for the use of his Spex fluorolog.

JA963440S

(35) Henriksen, T.; Dahlback, A. D.; Larsen, S. H. H.; Moan, *J. Photochem. Photobiol.* **1990**, *51*, 579−582.

(36) Blum, H. F. *Photodynamic Action and Diseases Caused by Light*; Hafner: New York, 1964.